

# *In silico* Investigation of Potential Therapeutic Medication for the Inhibition of Dengue Virus (DENV NS2B/NS3 and NS1) by Modification of Polycyclic quaternary Alkaloid (Sanguinarine Derivatives) with Different Computational Approaches

Shopnil Akash<sup>1,\*</sup> , Fateha Arefin<sup>1</sup>, Farjana Islam Aovi<sup>1</sup> 

<sup>1</sup> Department of Pharmacy, Faculty of Allied Health Sciences, Daffodil International University, Dhaka 1207, Bangladesh shopnil.ph@gmail.com (S.A.); fatehah1548@gmail.com (F.A.); farjana.pharm@diu.edu.bd (F.I.A.);

\* Correspondence: shopnil.ph@gmail.com (S.A.);

Scopus Author ID 57475390700

Received: 10.08.2022; Accepted: 4.10.2022; Published: 16.11.2022

**Abstract:** Dengue fever, spread by mosquitoes, has emerged as one of the world's most significant infectious diseases. To replicate and generate more copies of itself inside the host cell, the virus needs its proteins. With the NS2B cofactor, the NS3 protease can convert the polyprotein into functional proteins. As a result, NS3 protease is an attractive target for researching and developing antiviral drugs to combat the dengue virus. So, To develop efficient antagonists against the NS2B/NS3 and NS1 protein, a comprehensive screening integrates ADMET properties, molecular docking, and QSAR investigation is carried out against NS2B/NS3 (PDB ID 3L6P) and NS1 (PDB ID 4O6B) for the potential targeted region. ADMET characteristics analysis was performed to screen (01- 09) antiviral polycyclic quaternary alkaloids (sanguinarine derivatives) to identify ligands that contravene absorption, distribution, metabolism, excretion, and toxicity (ADMET) parameters. From the outcome of the docking investigation, the binding energy is reported as -8.5 kcal/mole as the lowest and - 9.7 kcal/mole as the highest with NS2B/NS3 (PDB ID 3L6P) and -9.8 kcal/mole, -9.9 kcal/mole, -10.0 kcal/mole, -10.2 kcal/mole in ligands 06, 03,07 and 09 against NS1 (PDB ID 4O6B). It is noted that their solubility was determined to be moderate in the water system, and absorption rates were exceptionally high in the GI tract. None of the molecules were harmful to the liver (hepatotoxic) or skin sensitization. The predicted QSAR and pIC50 value and Lipinski rule are also accepted within the standard ranges. Therefore, the estimated *in silico* different biochemical score for the polycyclic quaternary alkaloid (sanguinarine derivatives) towards NS2B/NS3 (PDB ID 3L6P) and NS1 (PDB ID 4O6B) inhibitors suggests that these compounds could have a high level of efficacy.

**Keywords:** dengue; molecular docking; drug-likeness; ADMET; QSAR.

© 2022 by the authors. This article is an open-access article distributed under the terms and conditions of the Creative Commons Attribution (CC BY) license (<https://creativecommons.org/licenses/by/4.0/>).

## 1. Introduction

The coronavirus infection (SARS-CoV-2) has led the world in the last couple of years. More than 589,678,215 people had been infected, and 6,437,085 people died by August 8, 2022 [1,2], and the world health organization designated a global pandemic on a global scale on March 11, 2020 [3-5]. This epidemic is continuing and causing widespread destruction around the globe at the same time as several nations have been dealing with an outbreak of dengue

fever, a well-known tropical illness [6]. So, this dengue fever makes a significant concern to the global policymaker [7,8].

Dengue fever mainly occurs due to a type of mosquito-borne viral illness. It is an RNA virus that consists of a single strand. The NS3 protease has six  $\beta$ -strands organized into two  $\beta$ -barrel geometries. It may generate 11 kilobase viral genome with a molecular weight of about 378 kilodaltons, which is then further translated by host cell protease and virus-encoded NS2B-NS3 protease into a total of three structural proteins (C, prM, and E) and seven non-structural proteins (NS1, NS2A, NS2B, NS3, NS4A, NS4B, and NS5)[7, 8].

In recent times, it has been a severe public health problem around the globe. The DENV-1 and DENV-2 viruses have been the most common ones, which have been seen in Bangladesh and the majority of Southeast Asian countries [9,10]. It spreads at the fastest rate of any other mosquito-borne virus. During the *SARS-CoV-2* pandemic, the rising prevalence of dengue infection became an additional hazard, particularly in the dengue-endemic regions of Southeast Asia and Latin America [11]. The impact of dengue fever on a worldwide scale is constantly shifting, with an estimated 50 million new cases occurring annually in around 100 nations [12,13]. Because most countries are now engaged in a war against COVID-19, any additional dengue breakout has caused several challenging logistical problems for those attempting to tackle both illnesses simultaneously. As a direct result, patients infected with coronavirus and dengue viral infection have been recorded lately in several countries, including India, Thailand, Singapore, and Bangladesh [14,15].

Consequently, it is hypothesized that the number of instances of co-infection will grow and be discovered in more nations in the following days as the dengue season reaches its highest. At the moment, many countries in South America, including Paraguay, Argentina, Colombia, and Bolivia, are experiencing severe epidemics of dengue and Covid-19 [16]. In addition, several nations in Southeast Asia, such as Indonesia, the Philippines, and Malaysia, are also experiencing the same co-epidemics [17]. Because of this, there is a chance that more people may get infected with dengue and coronavirus infection, particularly in these nations where the number of dengue and coronavirus infection patients has already reached an alarmingly high level. Therefore, the co-infection of *SARS-CoV-2* and dengue, as well as the epidemic of both diseases at the same time, has created an additional challenge for medical experts and imposed a significant burden on the health care system [18].

Many scientific research and reports project that there will be an additional 2.25 (1.27–2.80) billion individuals at risk of dengue infections in 2080[19], increasing the overall population at risk to around 6.1 (4.7–6.9) billion. This is almost 60 percent of the world's population [20]. But it is a matter of great concern that there is no potential medicine for fighting this life-threatening viral infection. So, the synthetic source might be an alternative option for designing and developing an effective agonist or medication for the inhibition of dengue. But this is a very much challenging job due to the great chances of failing during the pre-clinical phase; time-consuming and requires a huge amount of costs. So, the advanced virtual screening tool may enhance the probability of success rate and reduce both time and cost. This is why this study is designed by structural modification of polycyclic quaternary alkaloids (sanguinarine derivatives). Numerous scientific research has demonstrated this alkaloid to have antibacterial, antioxidant, anti-inflammatory, and anti-tumor properties [21,22]. So, it is motivated to investigate the efficiency of antiviral medication against the dengue virus. The main objective of this investigation is to determine how different functional

groups impact the pharmacological efficacy of these modified derivatives against the dengue virus.

## 2. Materials and Methods

### 2.1. Optimization and ligand preparation.

Figure 1 displays the optimized structures of sanguinarine derivatives (01-09). The geometries of these chemical polycyclic quaternary alkaloids (sanguinarine derivatives) (01-09) were developed by Hyperchem and extensively optimized by the use of the Gaussian 09 program at the B3LYP/6-311G+(d,p) level [23].

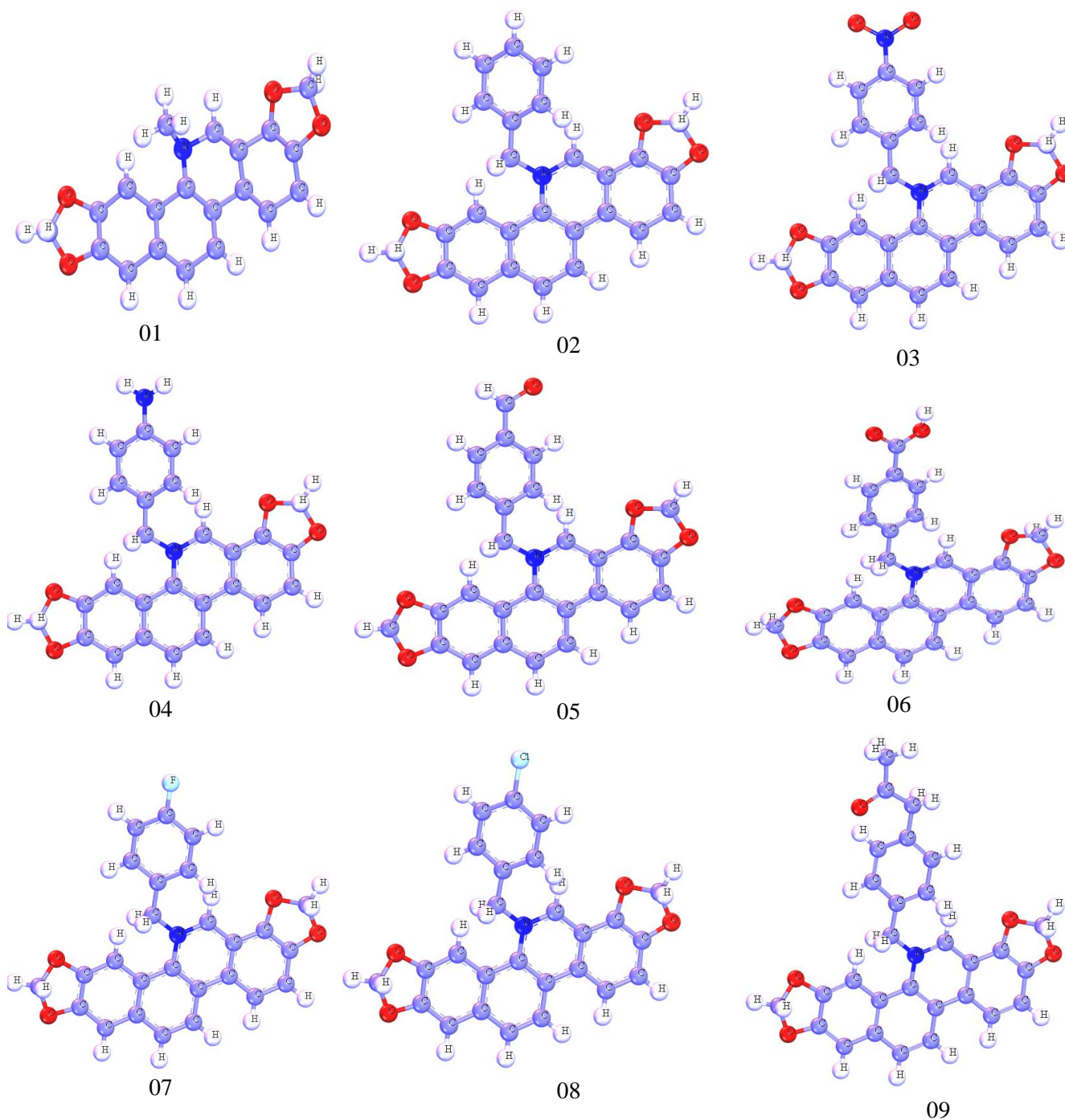


**Figure 1.** optimized structures of sanguinarine derivatives.

DFT was used with Becke's method to carry out the comprehensive geometry optimization and following vibrational frequency calculations (B). Once the optimization is done, they have been exported as pdb file types, and the 3d view of the images is collected and displayed below. These pdb-exported files were then used for molecular docking, ADMET, pharmacokinetics, and other computational performance.

### 2.2. *In silico* ADMET.

The absorption, distribution, metabolism, excretion, and toxicity (ADMET) properties of the (01-09) sanguinarine derivatives were collected from pkCSM (<https://biosig.lab.uq.edu.au/pkcsm/>) and admetSAR (<http://lmmd.ecust.edu.cn/admetSar1>) server. These two websites are considered one of the most well-known sources for virtual screening molecular ADMET properties prediction [24,25].

### 2.3. Protein purification and method for molecular docking.

The elevated crystal structure of the dengue virus NS2B/NS3 protease was obtained from the RCSB protein data bank (PDB-ID: 3L6P); Resolution: 2.20 Å; Method: X-RAY DIFFRACTION; Organism: dengue virus 1; and NS1 (PDB ID 4O6B); Resolution: 3.00 Å; Method: X-RAY DIFFRACTION and Organism: dengue virus 2 [26,27]. In Swiss-PDB Viewer, the crystalline structure of DENV NS2B/NS3 and NS1 was optimized to reduce and minimize excess energy [28]. The protein structure revealed several crucial aspects, including missing hydrogen, incorrect bond order, and side-chain shape, which has been corrected and removed the excess molecules such as water and hetero atom to get a purified protein. Then, these proteins were exported in PDB format. Then, the virtual screening technique was accomplished in AutoDock Vina, outfitted with PyRx virtual screening for molecular docking[29,30].

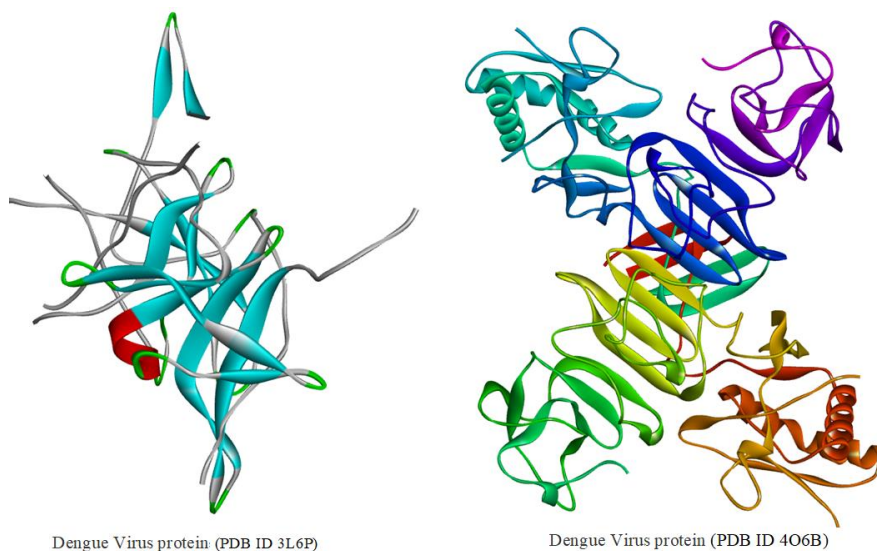


**Figure 2.** Three-dimensional protein structure of dengue species.

The purified protein was uploaded in PyRx AutoDock software during molecular docking procedures and converted into macromolecules. Similarly, previously prepared ligands were uploaded, minimizing the energy, and converted as autodock ligands. The grid center points were set to X = -21.6534, Y = -17.1288, Z = 25.1838, and the box dimensions (Å) X = 47.70331, Y = 64.6083, Z = 51.65096 for (PDB-ID: 3L6P), and the grid center for (PDB ID 4O6B); X = -8.7259, Y = -31.6119, Z = -27.5813, and box dimension X = 81.3565, Y =

55.5874 and Z= 91.9504 Grid box parameters were set to wrap the substrate-binding pocket of the protein. In Fig.2, the three-dimensional structures of the protein are shown.

#### 2.4. QSAR and $pIC_{50}$ calculation.

Quantitative structure-activity relationship (QSAR) approaches are very significant in determining the bioactivity of target compounds premised on mathematical and statistical linkages [31]. In this study, we built a multiple linear regression model (MLR) of drugs that inhibit the DENV NS2B/NS3 and NS1 protease. The model was generated based on previous research [32]. Furthermore, this MLR model has been applied to analyze the biological activity of the sanguinarine derivatives. Before that, the statistical QSAR model was stimulated in excel 2020, based on multiple linear regression, and all the required data were taken from "(<http://www.scbdd.com/chemdes/>)"[33].

### 3. Result and Discussion

#### 3.1. Structural activity relationship.

The structure-activity relationship (SAR) is a wonderful method for drug development, from assessing drug targets to improving a molecule's features.

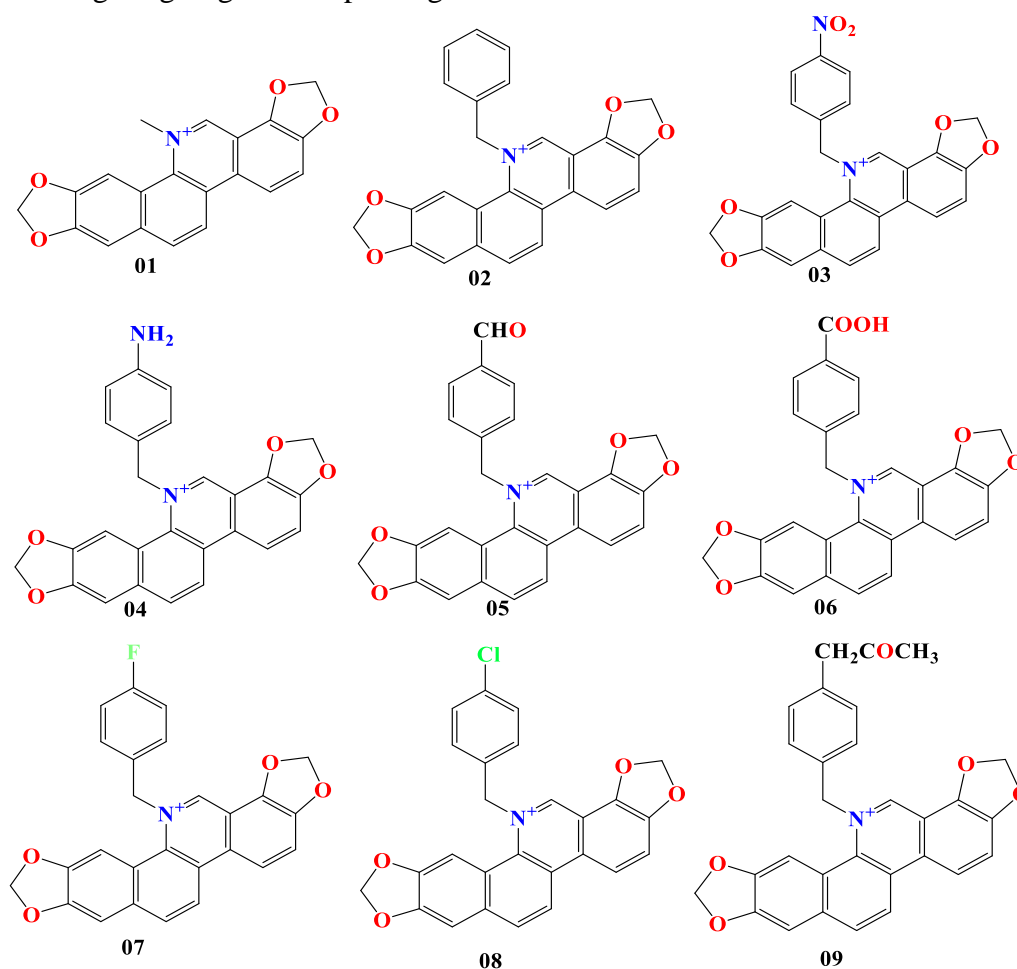


**Figure 3.** Chemical structure of sanguinarine and its derivatives.

Different geometric and electrostatic interactions contribute to efficient bioactivity by adding or deleting the functional group [34]. So, to develop a potential inhibitor and get the desired efficiency against DENV NS2B/NS3 and NS1 protein. The polycyclic quaternary

alkaloid (sanguinarine derivatives) was selected, and with the addition of eight different functional groups, these molecules were transferred for further computational evaluation.

### 3.2. Lipinski rule, pharmacokinetics.

The Lipinski Rule of 5' (RO5) announcement by Lipinski in 1997 was among the most impactful contemporary pharmacological studies [35]. Different fractions have improved and extended the RO5 and promised new guidelines to drive drug design initiatives nearly fifteen years after the announcement of the initial RO5 study. This guideline was designed and established based on five rules, and any drug molecules accepted by RO5 should be considered as potential medication. This guideline included; the partition coefficient log P range should be -0.4 to +5.6, and Molecular reactivity ranging from 40 to 130. Lipinski's rule is crucial in drug development when a biologically active lead structure is improved step-wise to maximize activity and selectivity while maintaining drug-like physical features. Physicochemical indicators and the *in silico* Lipinski Rule of Five may quantify drug-like characteristics. It could also be employed during drug development to screen libraries for compounds and exclude those with low potential [36]. Molecular weight in the range of 180 to 480, and Count of molecules ranging from 20 to 70 (this encompasses, H-bond donors like O and N, as well as H-bond acceptors) [37]. The online data set SwissADME is used to predict this Lipinski value, and the calculated data are listed in Table 1.

The obtained value reported that ranging of molecular weight 332 Dalton – 464 Dalton, Number of rotatable bonds 0-04, Hydrogen bond acceptor 04 -06, Hydrogen bond donor maximum 01, Molar Refractivity 94.68 – 127 excluding Ligand 09, and partition coefficient log (P) 2.88 -4.66. They have mentioned that ligands (01-09) have a similar bioavailability index. So, according to the acquired data, they all accepted the Lipinski guidelines.

**Table 1.** Data on the Lipinski rule, pharmacokinetics, and Drug likeness.

| Ligand No | Molecular weight | Number of rotatable bonds | Hydrogen bond acceptor | Hydrogen bond donor | Molar Refractivity | partition coefficient log P | Lipinski rule |           | Bioavailability Score |
|-----------|------------------|---------------------------|------------------------|---------------------|--------------------|-----------------------------|---------------|-----------|-----------------------|
|           |                  |                           |                        |                     |                    |                             | Result        | violation |                       |
| 01        | 332.33           | 00                        | 04                     | 00                  | 94.68              | 2.88                        | Yes           | 00        | 0.55                  |
| 02        | 408.43           | 02                        | 04                     | 00                  | 119.16             | 4.14                        | Yes           | 00        | 0.55                  |
| 03        | 453.42           | 03                        | 06                     | 00                  | 127.99             | 3.48                        | Yes           | 00        | 0.55                  |
| 04        | 423.44           | 02                        | 04                     | 01                  | 123.57             | 3.61                        | Yes           | 00        | 0.55                  |
| 05        | 436.44           | 03                        | 05                     | 00                  | 124.55             | 3.79                        | Yes           | 00        | 0.55                  |
| 06        | 452.43           | 03                        | 06                     | 01                  | 16.12              | 3.66                        | Yes           | 00        | 0.55                  |
| 07        | 426.42           | 02                        | 05                     | 00                  | 119.12             | 4.42                        | Yes           | 00        | 0.55                  |
| 08        | 442.87           | 02                        | 04                     | 00                  | 124.17             | 4.66                        | Yes           | 00        | 0.55                  |
| 09        | 464.49           | 04                        | 05                     | 00                  | 133.34             | 4.21                        | Yes           | 00        | 0.55                  |

### 3.3. Molecular docking against dengue virus (DENV NS2B/NS3 and NS1).

The molecular docking investigation was undertaken to identify the strong interaction (Binding Affinity) responsible for the developed capability to attach to the targeted protein of interest [38,39]. In this investigation, the DENV NS2B/NS3 and NS1 proteins functioned as candidates for the ligand binding or targeted receptor. Generally, a criterion of -6.00 kcal/mole is acceptable for prospective medications [40,41]. The binding affinities were computed using

the kcal/mole unit, which implies that a substantial negative result indicates stronger interaction between the ligand and the targeted protein.

In our investigation against DENV NS2B/NS3 and NS1, the binding energy is found to be -8.5 kcal/mole, the lowest, and -9.7 kcal/mole as the highest with NS2B/NS3 (PDB ID 3L6P). The efficiency was reported as a better result for NS2B/NS3 (PDB ID 3L6P). We have targeted another binding site of the dengue virus, such as NS1 (PDB ID 4O6B). This time, the binding energy is reported much better than the NS2B/NS3 (PDB ID 3L6P). Specifically, -9.8 kcal/mole, -9.9 kcal/mole, -10.0 kcal/mole, and -10.2 kcal/mole in ligands 06, 03, 07, and 09. So, here it is noted that -COOH, NO<sub>2</sub>, Cl, and CH<sub>2</sub>COCH<sub>3</sub> greatly impact binding energy. Our primary goal was to improve the efficiency of drug-like properties by modifying polycyclic quaternary alkaloids (sanguinarine derivatives), which has been satisfied.

**Table 2.** Virtual screening and molecular docking score.

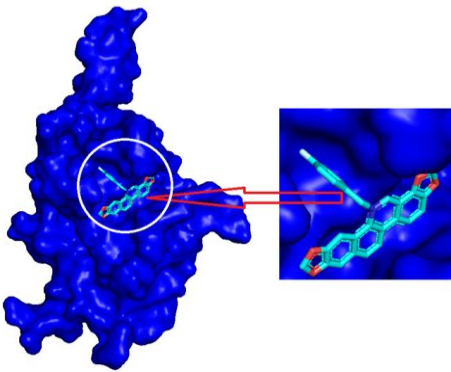
| Drug Molecules No | Binding Affinity against DENV NS2B/NS3 and NS1 |  |
|-------------------|--|--|
|                   | Dengue Virus protease NS2B/NS3 (PDB ID 3L6P)   | Dengue Virus protein NS1 (PDB ID 4O6B) |
|                   | Binding Affinity(kcal/mole)                    | Binding Affinity(kcal/mole)            |
| 01                | -8.5   | -9.0                                   |
| 02                | -9.0   | -9.4                                   |
| 03                | -9.1   | -9.9                                   |
| 04                | -8.9   | -9.6                                   |
| 05                | -8.8   | -9.5                                   |
| 06                | -9.3   | -9.8                                   |
| 07                | -9.7   | -10.0                                  |
| 08                | -9.5   | -9.8                                   |
| 09                | -9.2   | -10.2                                  |

#### 3.4. Protein-ligand interaction and molecular docking pose.

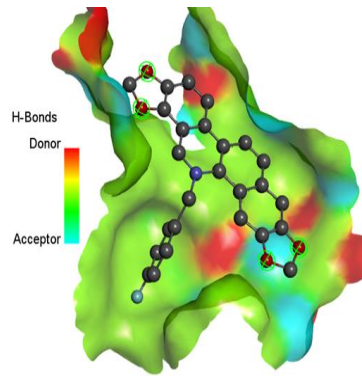
The BIOVIA Discovery Studio Visualizer was applied to investigate the extent of the non-covalent interactions between the ligands and the protein[42]. Non-covalent interactions, including hydrogen bonding and hydrophobic interactions, are responsible for a significant role in stabilizing energetically favorable ligands at the active site of a targeted macromolecular structure, enhancing increased binding affinity and medication effectiveness. Therefore, in an attempt to comprehend that the protein-ligand complex system was maintained in a stable state throughout the MD simulation. This experiment has been performed, analyzing and comparing the stabilization of these connections in the conceptual model.

In protein ligands binding pocket, it is clearly seen how they engaged with each other during the formation of complex molecules. Consequently, amino acid residues that function during the interaction may constitute the most significant key factor in determining the binding affinity of protein-ligand complexes. Then, the hydrogen bonding donor or acceptor region is evaluated, where the red color is the donor region, and the sky-blue color indicates the acceptor region. Finally, a 2D image of active amino acids illustrates where different amino acid types are present with different bond angles. These amino acid residues are generated during the formation of drug-protein complexes, which include PHE-166, VAL-173, VAL-212, GLY-203, ASN-234, LEU-206, PRO-226, LYS-227, and GLY-203, A: GLY-203, A: VAL-173, A: VAL-204, A: VAL-212, A: PHE-166, A: ALA-214, A: ALA-214, A: ALA-216, A: LYS-124.

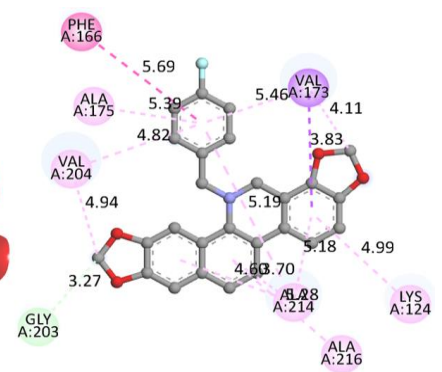
**Protein ligands binding pocket**



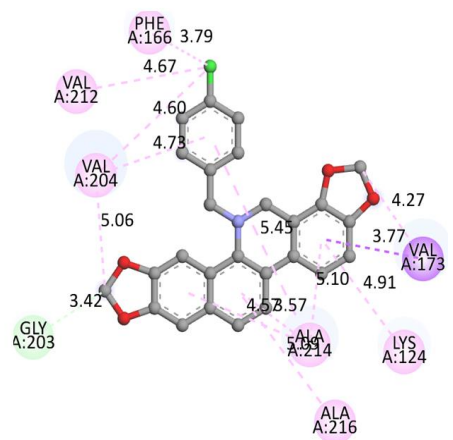
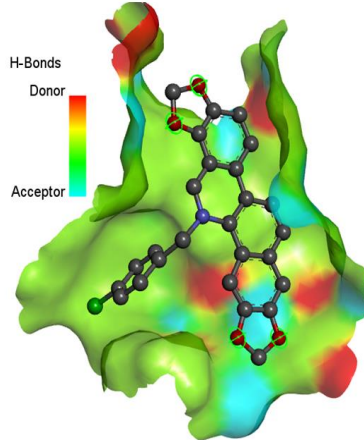
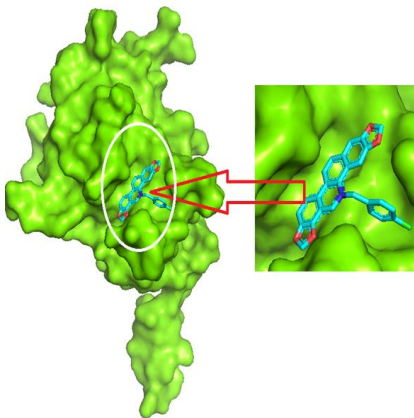
**Hydrogen bonding**



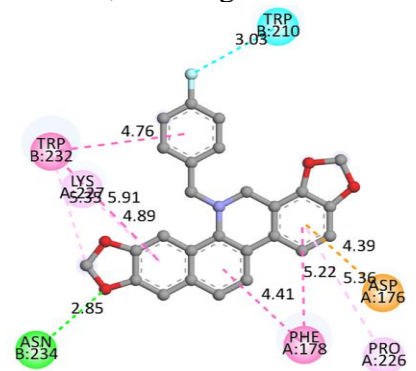
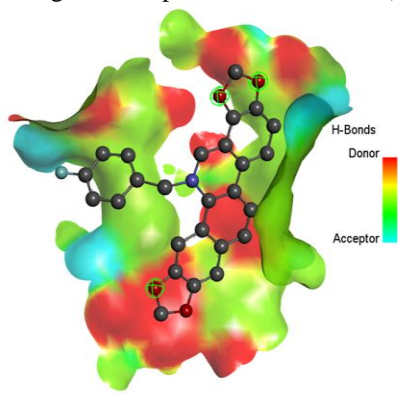
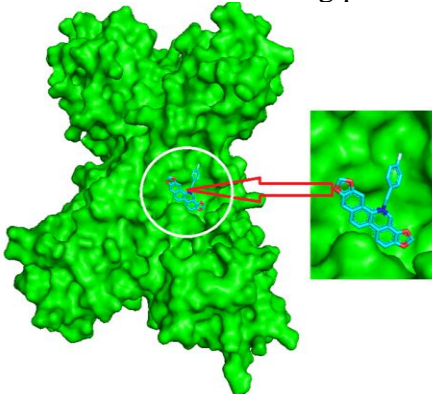
**2D picture of active sites.**



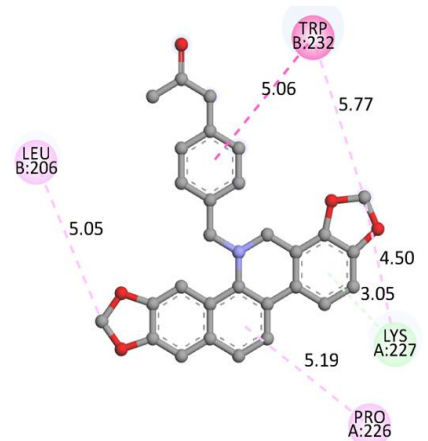
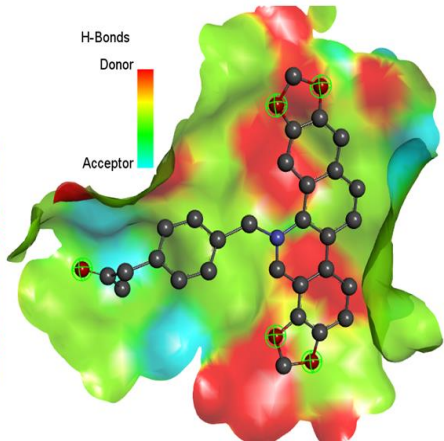
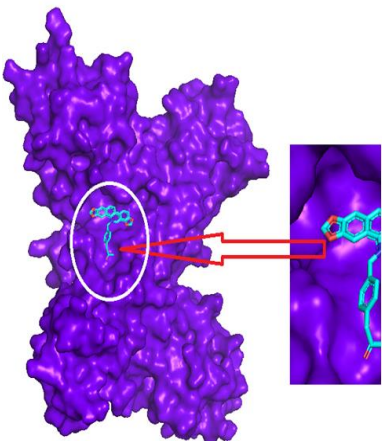
**Molecular docking poses of Dengue Virus protease NS2B/NS3 (PDB ID 3L6P) with Ligand 07**



**Molecular docking poses of Dengue Virus protease NS2B/NS3 (PDB ID 3L6P) with Ligand 08**



**Molecular docking poses of Dengue Virus protein NS1 (PDB ID 4O6B) with Ligand 07**



**Molecular docking poses of Dengue Virus protein NS1 (PDB ID 4O6B) with Ligand 09**



**Figure 4.** Docking interactions between the proposed compound and DENV NS2B/NS3 and NS1.

### 3.5. Solvent accessible surface (SAS) ionizability and aromaticity analysis.

#### 3.5.1. Solvent surface area.

The efficiency of biomolecules that may be dissolved in solvents is a factor that significantly affects the structure and function of biological molecules [43]. This functionality of biomolecules depends heavily on solvent accessibility [44]. In most cases, the amino acid residues found on the surface of a protein function as active sites and interact with other macromolecules and bioactive compounds. The essential characteristics of the solvent accessibility of amino acid residues, and nucleotides, in biomaterials complexes play a significant aspect in the durability and stability of biological macromolecules. This section has explained how to anticipate a molecule's solvent accessibility based on its three-dimensional structure and amino acid sequence. In Figure 5(a), the color blue represents an area with a greater volume of solvent-accessible surface (SAS). In contrast, the green color depicts a region with a lesser density of the solvent-accessible surface. The SAS region of all development molecules is much higher than the lower region.

#### 3.5.2. Ionizability.

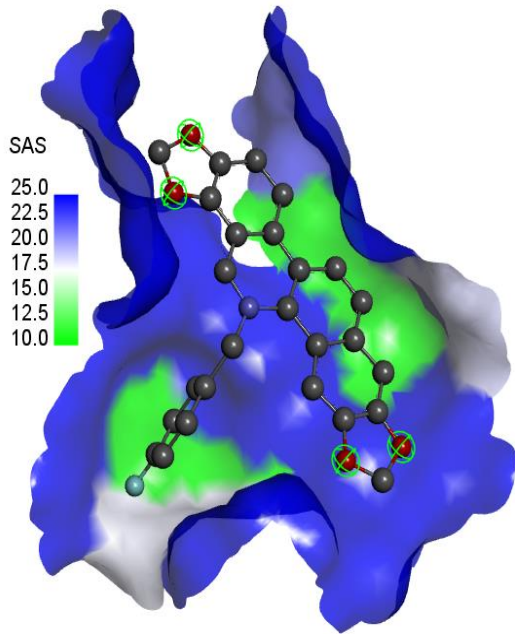
The medication's lipid permeability, preparation, and administration approach all influence how well a drug is absorbed [45]. In the absence of an active transport mechanism or the drug is so microscopic that it can pass through the aqueous pathways in the transmembrane, medication must be lipophilic to be capable of entering cell walls. Most medicines belonging to the middle group are absorbed into the body's overall water content. Because just the unionized medication is lipid-soluble, absorption and distribution of drugs that are just slightly acidic or slightly basic depend on the pH. Ionized medications cannot pass across barriers, meaning they cannot be absorbed systemically and cannot penetrate the membrane that separates the bloodstream from the brain or BBB [46]. Therefore, it is not possible to reach the desired adequate quantities of the medicine at the location where it is working or targeted organ

In Figure 5(b), the red color measured the basicity, and the sky-blue color measured acidic similarly; blue indicates the middle portion between the ionized and unionized condition. According to the finding, all the medications should be unionized, which means they can effectively absorb and achieve optimum efficiency at the therapeutic level. So, the drug should be unionized to achieve optimum efficiency.

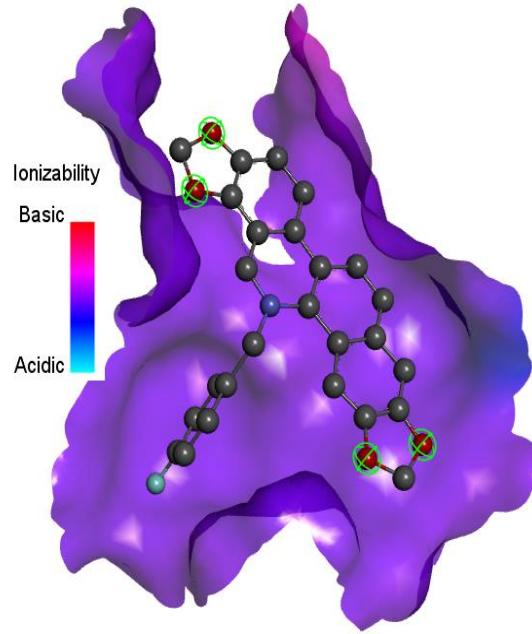
### 3.6. Quantitative structure-activity relationship (QSAR).

Statistical method quantitative structure-activity relationships are used to establish a correlation between a chemical structure and its bioactivity. In addition to predicting the properties of unstudied compounds, the QSAR model may be used for a comprehensive range function, such as the forecast of functions of compounds. In recent times, QSAR methodologies have received extensive scientific attention, notably in the pharmaceutical industry for drug development and toxicology, and are essential for drug discovery [47]. It has been hypothesized that drug compounds should be considered active whenever their pIC<sub>50</sub> value is greater than 10 [48].

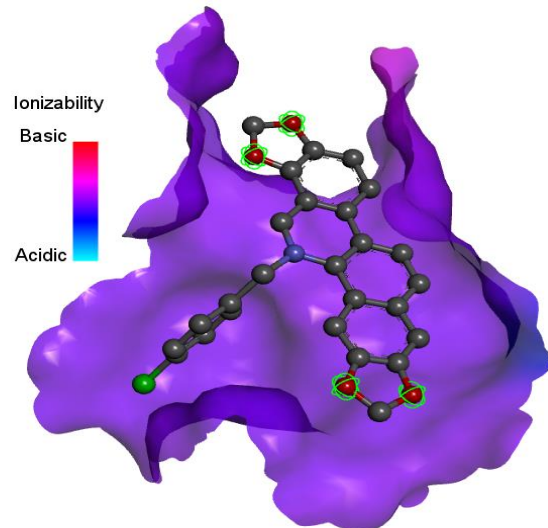
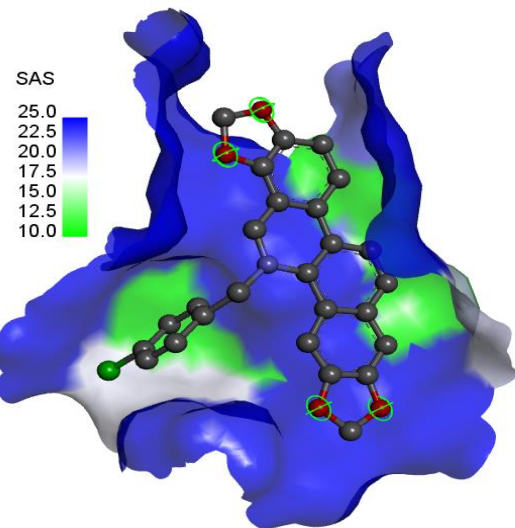
Solvent Accessible Surface 5 (a)



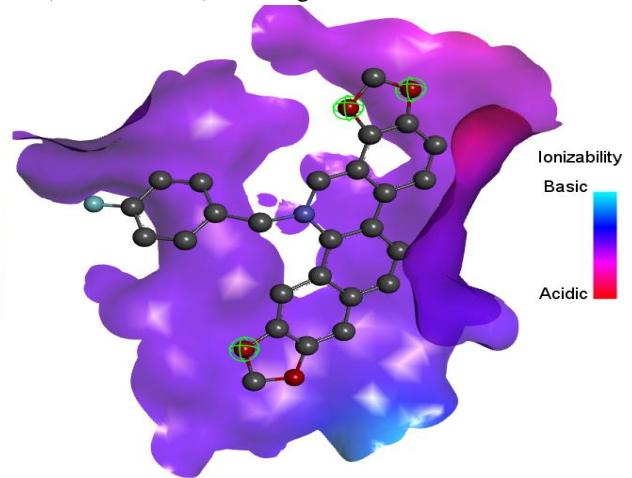
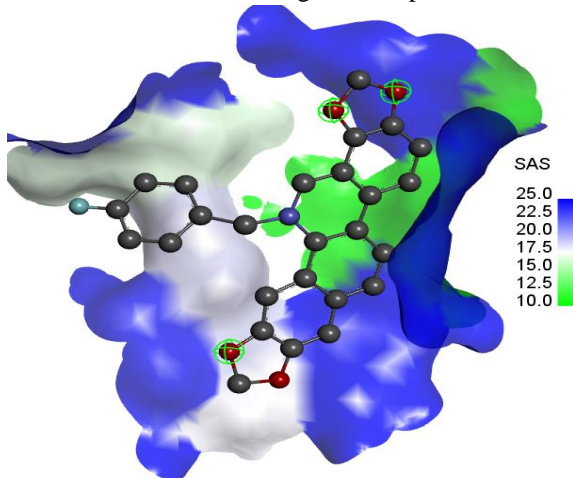
Ionizability 5 (b)



Dengue Virus protease NS2B/NS3 (PDB ID 3L6P) with Ligand 07



Dengue Virus protease NS2B/NS3 (PDB ID 3L6P) with Ligand 08



Dengue Virus protein NS1 (PDB ID 4O6B) with Ligand 07

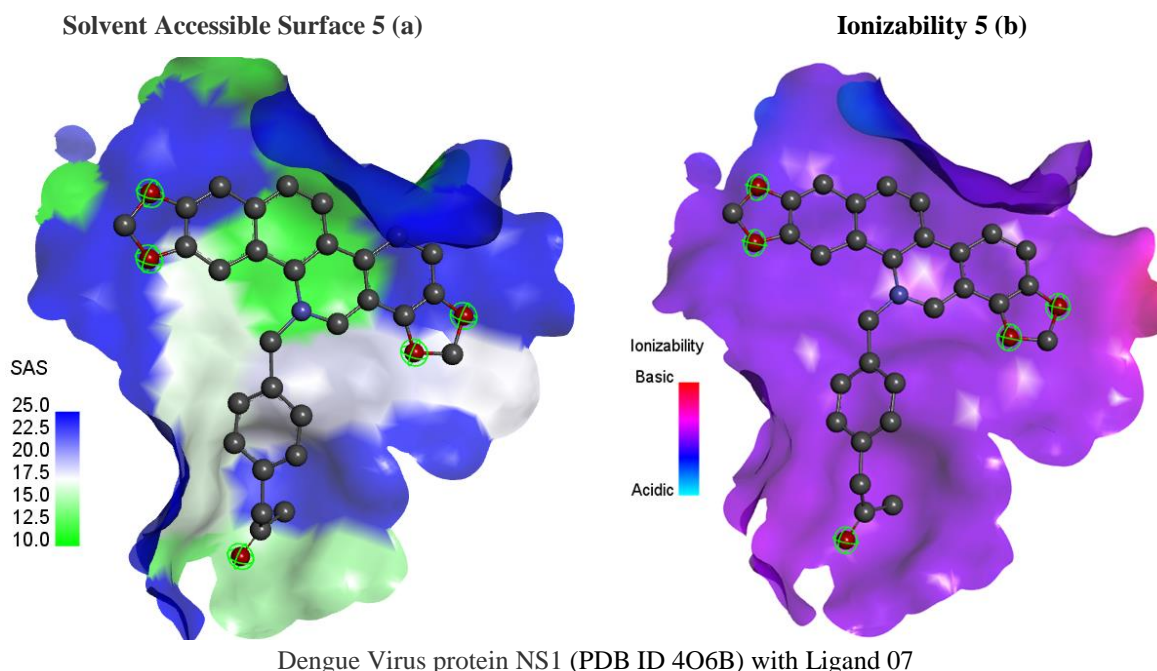


**Figure 5.** Graphical illustration of solvent-accessible surface (SAS) and ionizability analysis.

The computation of QSAR is carried out by using multiple linear regression (MLR). Following MLR equation was obtained from previous research[49,50], here,  $pIC_{50}$  (Activity) =  $- 2.768483965 + 0.133928895 \times (Chiv5) + 1.59986423 \times (bcutm1) + (- 0.02309681) \times (MRVSA9) + (- 0.002946101) \times (MRVSA6) + (0.00671218) \times (PEOEVSA5) + (- 0.15963415) \times (GATSv4) + (0.207949857) \times (J) + (0.082568569) \times (Diametert)$ .

Before that, the following data were acquired from ChemDes ([www.scbdd.com/chemdes/](http://www.scbdd.com/chemdes/)), including Chiv5, bcutm1, MRVSA9, MRVSA6, PEOEVSA5, GATSv4, J and Diametert, and calculated the  $pIC_{50}$ . After calculating this data, it has been seen that the  $pIC_{50}$  value is lower than five in most of the molecules, and only ligand 05 has greater than 5; According to the findings overall, the  $pIC_{50}$  value that is the lowest is around 4.56, and the value that is the highest is 5.33. Therefore, it is possible to conclude that this bioactive polycyclic quaternary alkaloid (sanguinarine derivatives) may have the potential to be stable and may function well as a therapeutic.

**Table 3.** Data of QSAR.

| Ligand | Chiv5 | bcutm1 | MRVSA9 | MRVSA6 | PEOEVSA5 | GATSv4 | J     | Diametert | $pIC_{50}$ |
|--------|-------|--------|--------|--------|----------|--------|-------|-----------|------------|
| 01     | 2.846 | 4.215  | 32.448 | 42.595 | 6.0660   | 0.761  | 1.27  | 11        | 4.57       |
| 02     | 3.472 | 4.221  | 32.448 | 78.490 | 36.398   | 0.801  | 1.183 | 11        | 4.58       |
| 03     | 3.584 | 4.222  | 38.135 | 82.538 | 6.066    | 0.802  | 1.114 | 13        | 4.56       |
| 04     | 3.551 | 4.221  | 38.135 | 72.524 | 18.199   | 0.795  | 1.17  | 13        | 4.51       |
| 05     | 3.590 | 4.221  | 38.734 | 77.987 | 30.332   | 0.801  | 4.795 | 12        | 5.33       |
| 06     | 3.606 | 4.222  | 38.417 | 77.987 | 18.199   | 0.802  | 1.14  | 13        | 4.68       |
| 07     | 3.508 | 4.221  | 32.439 | 78.241 | 6.066    | 0.713  | 1.17  | 13        | 4.72       |
| 08     | 3.670 | 4.222  | 44.49  | 77.447 | 29.08    | 0.809  | 1.17  | 12        | 4.52       |
| 09     | 3.803 | 4.222  | 38.431 | 77.987 | 30.32    | 0.787  | 1.116 | 14        | 4.84       |

### 3.7. *In silico* ADMET data prediction.

In contemporary memory, the *in silico* absorption, distribution, metabolism, excretion, and toxicity (ADMET) characteristics of putative bioactive molecules have been utilized in drug development as a primary screening tool for the early stages of the discovery phase. Early screening of ADMET investigation may reduce the chance of failing during the clinical phase.

The pkCSM is one of the best sources for predicting these required ADMET data[25]. In this investigation, the aqueous solubility ranges are about -3.148 to -4.843, which means they are moderately soluble in water. The absorption rate is about 100% as the maximum and 97% as the minimum; these values indicate that they all are highly absorbed in the gastrointestinal tract (GI). The Caco-2 permeability values range vary from  $0.792 \times 10^{-6}$  to  $1.40 \times 10^{-6}$ . The medication distribution may reach the blood-brain barrier (BBB) without ligands 03 and 06, while the volume of distribution (VDss) ranges are about -0.053 log L/kg to 1.159 logs L/kg. In metabolism, only ligand 01 may inhibit the CYP450 1A2 inhibitor. The total clearance rate was reported as 0.872 ml/min/kg - 1.368 ml/min/kg, while the effect on renal OCT2 substrate. Finally, toxicity prediction found that they all are free from skin sensitization and hepatotoxicity, and the max. tolerated dose log 0.416 mg/kg/day - 0.526 mg/kg/day, which means a maximum of 0.526 mg/kg/day drug should be consumed.

**Table 4.** ADME and Toxicity prediction.

| S/N | Absorption                |                                    |                                    | Distribution |                         | Metabolism           |                      | Excretion                      |                         | Toxicity                                   |                    |                |
|-----|---------------------------|------------------------------------|------------------------------------|--------------|-------------------------|----------------------|----------------------|--------------------------------|-------------------------|--|--------------------|----------------|
|     | Water solubility<br>Log S | Caco-2<br>Permeability x $10^{-6}$ | Human Intestinal<br>Absorption (%) | VDss (human) | BBB<br>Permeability +/- | CYP450 1A2 inhibitor | CYP450 2C9 substrate | Total Clearance<br>(ml/min/kg) | Renal OCT2<br>substrate | Max. tolerated the dose<br>(log mg/kg/day) | Skin Sensitization | Hepatotoxicity |
| 01  | -4.843                    | 1.406                              | 100                                | -0.053       | +                       | Yes                  | No                   | 1.064                          | No                      | 0.416                                      | No                 | No             |
| 02  | -4.212                    | 0.792                              | 100                                | -0.927       | +                       | No                   | No                   | 1.21                           | No                      | 0.496                                      | No                 | No             |
| 03  | -4.655                    | 0.96                               | 99.075                             | -1.116       | -                       | No                   | No                   | 1.032                          | No                      | 0.496                                      | No                 | No             |
| 04  | -4.766                    | 0.96                               | 97.713                             | -1.02        | +                       | No                   | No                   | 1.325                          | No                      | 0.523                                      | No                 | No             |
| 05  | -4.815                    | 0.97                               | 100                                | -1.027       | +                       | No                   | No                   | 1.253                          | No                      | 0.519                                      | No                 | No             |
| 06  | -3.148                    | 0.911                              | 97.719                             | -1.02        | -                       | No                   | No                   | 0.872                          | No                      | 0.484                                      | No                 | No             |
| 07  | -4.435                    | 0.821                              | 99.41                              | -1.009       | +                       | No                   | No                   | 1.214                          | No                      | 0.524                                      | No                 | No             |
| 08  | -4.92                     | 0.820                              | 98.508                             | -0.045       | +                       | No                   | No                   | 1.207                          | No                      | 0.526                                      | No                 | No             |
| 09  | -3.860                    | 0.845                              | 100                                | -1.159       | +                       | No                   | No                   | 1.368                          | No                      | 0.511                                      | No                 | No             |

#### 4. Conclusions

This research monitored the inhibitory effect of the natural polycyclic quaternary alkaloid (sanguinarine derivatives) compounds against NS2B/NS3 (PDB ID 3L6P) and NS1 (PDB ID 4O6B) using possible advanced computational techniques such as molecular docking and MD modeling in addition to associated others *in silico* investigation which has become a significant health concern for millions of people all over the world. It was encountered that all of the hypothesized polycyclic quaternary alkaloids (sanguinarine derivatives) succeeded the ADMET test due to their appropriate pharmacokinetic features, indicating that they have prospective use as potential medication candidates. According to the results of the docking investigation, all of the ligands actively engage in binding to the NS2B/NS3 (PDB ID 3L6P) and NS1 (PDB ID 4O6B), even though their values of binding affinity range from moderate to high (-8.5 kcal/mole, as lowest and -9.7 kcal/mole as highest for NS2B/NS3 (PDB ID 3L6P) and -9.8 kcal/mole, -9.9 kcal/mole, -10.0 kcal/mole, -10.2 kcal/mole in ligands 06, 03, 07 and 09 against NS1 (PDB ID 4O6B)). This binding of the molecules will impede the reproduction of the dengue virus proteins. The obtaining QSAR and pIC<sub>50</sub> ranges are below 5.0 for most of the compounds, and only ligand 05 has greater than QSAR and pIC<sub>50</sub> 5.0. So, the mentioned ranges also follow the QSAR guideline. Also, all the drug candidates accepted drug-likeness

properties. Finally, mentioned *in silico* performance documented that all these molecules could be effective after reaching a biological system. In conclusion, this study found new bioactive molecules that may perform as high efficiency for inhibiting dengue virus obtained from polycyclic quaternary alkaloid (sanguinarine derivatives) against the main protease of DENV NS2B/NS3 and NS1.

## Funding

This research didn't receive any funds.

## Acknowledgments

The author thanks the department of Pharmacy, Daffodil International University, for encouraging us to perform this research.

## Conflicts of Interest

The authors declare no conflict of interest.

## References

1. Rauf, A.; Abu-Izneid, T.; Khalil, A.A.; Hafeez, N.; Olatunde, A.; Rahman, M.; Semwal, P.; Al-Awthan, Y.S.; Bahattab, O.S.; Khan, I.N. Nanoparticles in clinical trials of COVID-19: An update. *International Journal of Surgery* **2022**, 106818, <https://doi.org/10.1016/j.ijssu.2022.106818>.
2. Islam, M.; Rahman, M.; Ahasan, M.; Sarkar, N.; Akash, S.; Islam, M.; Islam, F.; Aktar, M.; Saeed, M.; Harun-Or-Rashid, M. The impact of mucormycosis (black fungus) on SARS-CoV-2-infected patients: at a glance. *Environmental Science and Pollution Research* **2022**, 1-26, <https://link.springer.com/article/10.1007/s11356-022-22204-8>.
3. Aovi, F.I.; Akash, S.; Islam, S.; Mitra, A. Lockdown: Prevalence Of Mental Illness During Covid-19 In Dhaka, bangladesh. *Journal Of Mechanics Of Continua And Mathematical Sciences* **2021**, 16.
4. Khan, M.A.; Smith, J.E.M. "Covibesity," a new pandemic. *Obesity medicine* **2020**, 19, 100282, <https://doi.org/10.1016%2Fj.obmed.2020.100282>.
5. Rahman, M.M.; Shohag, S.; Islam, M.R.; Akhter, S.; Mim, S.A.; Sharma, R.; Rauf, A. An Insight into COVID-19 and Traditional Herbs: Bangladesh Perspective. *Medicinal Chemistry (Shariqah (United Arab Emirates))* **2022**, <https://doi.org/10.2174/1573406418666220829144746>.
6. Ridwan, R. COVID-19 and dengue: a deadly duo. *Tropical Doctor* **2020**, 50, 270-272, <https://doi.org/10.1177/0049475520936874>.
7. Rahman, F.I.; Ether, S.A.; Islam, M.R. Upsurge of dengue prevalence during the third wave of COVID-19 pandemic in Bangladesh: pouring gasoline to fire. *Clinical Pathology* **2022**, 15, 2632010X221076068, <https://doi.org/10.1177/2632010x221076068>.
8. Kulkarni, M.A.; Duguay, C.; Ost, K. Charting the evidence for climate change impacts on the global spread of malaria and dengue and adaptive responses: a scoping review of reviews. *Globalization and health* **2022**, 18, 1-18, <https://globalizationandhealth.biomedcentral.com/articles/10.1186/s12992-021-00793-2>.
9. Khan, M.; Saeed, A.; Al Mosabbir, A.; Raheem, E.; Ahmed, A.; Rouf, R.R.; Hasan, M.; Alam, F.B.; Hannan, N.; Yesmin, S. Clinical spectrum and predictors of severity of dengue among children in 2019 outbreak: a multicenter hospital-based study in Bangladesh. *BMC pediatrics* **2021**, 21, 1-10, <https://bmcpediatr.biomedcentral.com/articles/10.1186/s12887-021-02947-y>.
10. Tsheten, T.; Gray, D.J.; Clements, A.C.; Wangdi, K. Epidemiology and challenges of dengue surveillance in the WHO South-East Asia Region. *Transactions of The Royal Society of Tropical Medicine and Hygiene* **2021**, 115, 583-599, <https://doi.org/10.1093/trstmh/traa158>.
11. Chen, Y.; Li, N.; Lourenço, J.; Wang, L.; Cazelles, B.; Dong, L.; Li, B.; Liu, Y.; Jit, M.; Bosse, N.I. Measuring the effects of COVID-19-related disruption on dengue transmission in southeast Asia and Latin America: a statistical modelling study. *The Lancet infectious diseases* **2022**, 22, 657-667, [https://www.thelancet.com/journals/laninf/article/PIIS1473-3099\(22\)00025-1/fulltext](https://www.thelancet.com/journals/laninf/article/PIIS1473-3099(22)00025-1/fulltext).
12. Boutayeb, A. The double burden of communicable and non-communicable diseases in developing countries. *Transactions of the Royal society of Tropical Medicine and Hygiene* **2006**, 100, 191-199, <https://doi.org/10.1016/j.trstmh.2005.07.021>.
13. Organization, W.H. Comprehensive guideline for prevention and control of dengue and dengue haemorrhagic fever. *World Health Organization* **2011**, <https://apps.who.int/iris/handle/10665/204894>.

14. Yan, G.; Lee, C.K.; Lam, L.T.; Yan, B.; Chua, Y.X.; Lim, A.Y.; Phang, K.F.; Kew, G.S.; Teng, H.; Ngai, C.H. Covert COVID-19 and false-positive dengue serology in Singapore. *The Lancet Infectious Diseases* **2020**, *20*, 536, [https://doi.org/10.1016/s1473-3099\(20\)30158-4](https://doi.org/10.1016/s1473-3099(20)30158-4).
15. Joob, B.; Wiwanitkit, V. COVID-19 can present with a rash and be mistaken for dengue. *Journal of the American Academy of Dermatology* **2020**, *82*, e177, <https://doi.org/10.1016/j.jaad.2020.03.036>.
16. Miah, M.A.; Husna, A. Coinfection, coepidemics of COVID-19, and dengue in dengue-endemic countries: A serious health concern. *Journal of Medical Virology* **2021**, *93*, 161, <https://doi.org/10.1002/jmv.26269>.
17. Yong, Y.K.; Wong, W.F.; Vignesh, R.; Chattopadhyay, I.; Velu, V.; Tan, H.Y.; Zhang, Y.; Larsson, M.; Shankar, E.M. Dengue Infection-Recent Advances in Disease Pathogenesis in the Era of COVID-19. *Frontiers in Immunology* **2022**, 3220, <https://doi.org/10.3389%2Ffimmu.2022.889196>.
18. Miah, M. Dengue outbreak during Covid-19 pandemic: a further challenge to the health professionals. *Bangladesh Med Res Counc Bull* **2020**, *46*, 145-146, [https://bmrcbd.org/Bulletin/bulletin\\_pdf/4602/4602\\_LetterToEditor.pdf](https://bmrcbd.org/Bulletin/bulletin_pdf/4602/4602_LetterToEditor.pdf).
19. Guha-Sapir, D.; Schimmer, B. Dengue fever: new paradigms for a changing epidemiology. *Emerging themes in epidemiology* **2005**, *2*, 1-10, <https://doi.org/10.1186%2F1742-7622-2-1>.
20. Messina, J.P.; Brady, O.J.; Golding, N.; Kraemer, M.U.; Wint, G.; Ray, S.E.; Pigott, D.M.; Shearer, F.M.; Johnson, K.; Earl, L. The current and future global distribution and population at risk of dengue. *Nature microbiology* **2019**, *4*, 1508-1515, <https://www.nature.com/articles/s41564-019-0476-8>.
21. Kuete, V. Health effects of alkaloids from African medicinal plants. In *Toxicological survey of African medicinal plants*; Elsevier: 2014; pp. 611-633, <https://doi.org/10.1016/B978-0-12-800018-2.00021-2>.
22. Miao, F.; Yang, X.-J.; Zhou, L.; Hu, H.-J.; Zheng, F.; Ding, X.-D.; Sun, D.-M.; Zhou, C.-D.; Sun, W. Structural modification of sanguinarine and chelerythrine and their antibacterial activity. *Natural product research* **2011**, *25*, 863-875, <https://doi.org/10.1080/14786419.2010.482055>.
23. Frisch, M.J. Gaussian 92, Revision E. 3. *Gaussian, Inc., Pittsburgh PA* **1992**.
24. Yang, H.; Lou, C.; Sun, L.; Li, J.; Cai, Y.; Wang, Z.; Li, W.; Liu, G.; Tang, Y. admetSAR 2.0: web-service for prediction and optimization of chemical ADMET properties. *Bioinformatics* **2019**, *35*, 1067-1069, <https://doi.org/10.1093/bioinformatics/bty707>.
25. Pires, D.E.; Blundell, T.L.; Ascher, D.B. pkCSM: predicting small-molecule pharmacokinetic and toxicity properties using graph-based signatures. *Journal of medicinal chemistry* **2015**, *58*, 4066-4072, <https://doi.org/10.1021/acs.jmedchem.5b00104>.
26. Chandramouli, S.; Joseph, J.S.; Daudenarde, S.; Gatchalian, J.; Cornillez-Ty, C.; Kuhn, P. Serotype-specific structural differences in the protease-cofactor complexes of the dengue virus family. *Journal of virology* **2010**, *84*, 3059-3067, <https://doi.org/10.1128%2FJVI.02044-09>.
27. Akey, D.L.; Brown, W.C.; Dutta, S.; Konwerski, J.; Jose, J.; Jurkiw, T.J.; DelProposto, J.; Ogata, C.M.; Skiniotis, G.; Kuhn, R.J. Flavivirus NS1 structures reveal surfaces for associations with membranes and the immune system. *Science* **2014**, *343*, 881-885, <https://doi.org/10.1126/science.1247749>.
28. Guex, N.; Peitsch, M.C. SWISS-MODEL and the Swiss-Pdb Viewer: an environment for comparative protein modeling. *electrophoresis* **1997**, *18*, 2714-2723, <https://doi.org/10.1002/elps.1150181505>.
29. Kumer, A.; Chakma, U.; Matin, M.M.; Akash, S.; Chando, A.; Howlader, D. The computational screening of inhibitor for black fungus and white fungus by D-glucofuranose derivatives using *in silico* and SAR study. *Organic Communications* **2021**, *14*, <https://search.bvsalud.org/global-literature-on-novel-coronavirus-2019-ncov/resource/en/covidwho-1614497>.
30. Morris, G.M.; Goodsell, D.S.; Huey, R.; Hart, W.E.; Halliday, S.; Belew, R.; Olson, A.J. AutoDock. *Automated docking of flexible ligands to receptor-User Guide* **2001**, [https://autodock.scripps.edu/wp-content/uploads/sites/56/2022/04/AutoDock3.0.5\\_UserGuide.pdf](https://autodock.scripps.edu/wp-content/uploads/sites/56/2022/04/AutoDock3.0.5_UserGuide.pdf).
31. Dearden, J.C. The history and development of quantitative structure-activity relationships (QSARs). In *Oncology: breakthroughs in research and practice*; IGI Global: 2017; pp. 67-117, <https://doi.org/10.4018/IJQSPR.2016010101>.
32. Siddiquey, F.; Roni, M.; Kumer, A.; Chakma, U.; Matin, M. Computational investigation of Betalain derivatives as natural inhibitor against food borne bacteria. *Current Chemistry Letters* **2022**, *11*, 309-320, <http://dx.doi.org/10.5267/j.ccl.2022.3.003>.
33. Wang, Y.-L.; Li, J.-Y.; Shi, X.-X.; Wang, Z.; Hao, G.-F.; Yang, G.-F. Web-Based Quantitative Structure-Activity Relationship Resources Facilitate Effective Drug Discovery. *Topics in Current Chemistry* **2021**, *379*, 1-24, <https://doi.org/10.1007/s41061-021-00349-3>.
34. Gianti, E.; Zauhar, R.J. Structure-activity relationships and drug design. In *Remington*; Elsevier: 2021; pp. 129-153, <https://doi.org/10.1016/B978-0-12-820007-0.00007-6>.
35. Walters, W.P. Going further than Lipinski's rule in drug design. *Expert opinion on drug discovery* **2012**, *7*, 99-107, <https://doi.org/10.1517/17460441.2012.648612>.
36. Hill, R.; Kenakin, T.; Blackburn, T. *Pharmacology for Chemists: Drug Discovery in Context*; Royal Society of Chemistry: **2017**, ([https://books.google.com.bd/books?hl=en&lr=&id=g-Y7DwAAQBAJ&oi=fnd&pg=PA79&dq=Hill,+R.%3B+Kenakin,+T.%3B+Blackburn,+T.+Pharmacology+for+Chemists:+Drug+Discovery+in+Context%3B+Royal+Society+of+Chemistry:+2017&ots=6ZSc-clUu7&sig=npCCQsxtZ2DNjo4LH\\_TIzRPyJNk&redir\\_esc=y#v=onepage&q=Hill%2C%20R.%3B%20Ke](https://books.google.com.bd/books?hl=en&lr=&id=g-Y7DwAAQBAJ&oi=fnd&pg=PA79&dq=Hill,+R.%3B+Kenakin,+T.%3B+Blackburn,+T.+Pharmacology+for+Chemists:+Drug+Discovery+in+Context%3B+Royal+Society+of+Chemistry:+2017&ots=6ZSc-clUu7&sig=npCCQsxtZ2DNjo4LH_TIzRPyJNk&redir_esc=y#v=onepage&q=Hill%2C%20R.%3B%20Ke)

- nakin%2C%20T.%3B%20Blackburn%2C%20T.%20Pharmacology%20for%20Chemists%3A%20Drug%20Discovery%20in%20Context%3B%20Royal%20Society%20of%20Chemistry%3A%202017&f=false)
37. Lipinski, C.A. Lead-and drug-like compounds: the rule-of-five revolution. *Drug discovery today: Technologies* **2004**, *1*, 337-341, <https://doi.org/10.1016/j.ddtec.2004.11.007>.
  38. El-Helby, A.G.A.; Ayyad, R.R.; Zayed, M.F.; Abulkhair, H.S.; Elkady, H.; El-Adl, K. Design, synthesis, *in silico* ADMET profile and GABA-A docking of novel phthalazines as potent anticonvulsants. *Archiv Der Pharmazie* **2019**, *352*, 1800387, <https://doi.org/10.1002/ardp.201800387>.
  39. Elkaeed, E.B.; Elkady, H.; Belal, A.; Alsouk, B.A.; Ibrahim, T.H.; Abdelmoaty, M.; Arafa, R.K.; Metwaly, A.M.; Eissa, I.H. Multi-Phase *In silico* Discovery of Potential SARS-CoV-2 RNA-Dependent RNA Polymerase Inhibitors among 3009 Clinical and FDA-Approved Related Drugs. *Processes* **2022**, *10*, 530, <https://doi.org/10.3390/pr10030530>.
  40. Kawsar, S.; Kumer, A.; Munia, N.S.; Hosen, M.A.; Chakma, U.; Akash, S. Chemical descriptors, PASS, molecular docking, molecular dynamics and ADMET predictions of glucopyranoside derivatives as inhibitors to bacteria and fungi growth. *Organic Communications* **2022**, *15*, <http://dx.doi.org/10.25135/acg.oc.122.2203.2397>.
  41. Kumer, A.; Chakma, U.; Rana, M.M.; Chandro, A.; Akash, S.; Elseehy, M.M.; Albogami, S.; El-Shehawi, A.M. Investigation of the New Inhibitors by Sulfadiazine and Modified Derivatives of  $\alpha$ -D-glucopyranoside for White Spot Syndrome Virus Disease of Shrimp by *In silico*: Quantum Calculations, Molecular Docking, ADMET and Molecular Dynamics Study. *Molecules* **2022**, *27*, 3694, <https://doi.org/10.3390/molecules27123694>.
  42. Tatar, G.; Ozyurt, E.; Turhan, K. Computational drug repurposing study of the RNA binding domain of SARS-CoV-2 nucleocapsid protein with antiviral agents. *Biotechnology progress* **2021**, *37*, e3110, <https://doi.org/10.1002/btpr.3110>
  43. Abel, R.; Young, T.; Farid, R.; Berne, B.J.; Friesner, R.A. Role of the active-site solvent in the thermodynamics of factor Xa ligand binding. *Journal of the American Chemical Society* **2008**, *130*, 2817-2831, <https://doi.org/10.1021/ja0771033>.
  44. Orozco, M.; Luque, F.J. Theoretical methods for the description of the solvent effect in biomolecular systems. *Chemical Reviews* **2000**, *100*, 4187-4226, <https://doi.org/10.1021/cr990052a>.
  45. Dahan, A.; Hoffman, A. The effect of different lipid based formulations on the oral absorption of lipophilic drugs: the ability of *in vitro* lipolysis and consecutive ex vivo intestinal permeability data to predict *in vivo* bioavailability in rats. *European journal of pharmaceuticals and biopharmaceutics* **2007**, *67*, 96-105, <https://doi.org/10.1016/j.ejpb.2007.01.017>.
  46. Pleuvry, B.J. Factors affecting drug absorption and distribution. *Anaesthesia & Intensive Care Medicine* **2005**, *6*, 135-138, <https://doi.org/10.1383/anes.6.4.135.63632>.
  47. Perkins, R.; Fang, H.; Tong, W.; Welsh, W.J. Quantitative structure-activity relationship methods: Perspectives on drug discovery and toxicology. *Environmental Toxicology and Chemistry: An International Journal* **2003**, *22*, 1666-1679, <https://doi.org/10.1897/01-171>.
  48. Rahman, M.A.; Matin, M.M.; Kumer, A.; Chakma, U.; Rahman, M.J.P.C.R. Modified D-Glucofuranoses as New Black Fungus Protease Inhibitors: Computational Screening, Docking, Dynamics, and QSAR Study. **2022**, *10*, 195-209, <https://doi.org/10.22036/PCR.2021.294078.1934>.
  49. De Oliveira, D.B.; Gaudio, A.C. BuildQSAR: a new computer program for QSAR analysis. *Quantitative Structure-Activity Relationships: An International Journal Devoted to Fundamental and Practical Aspects of Electroanalysis* **2000**, *19*, 599-601, [https://doi.org/10.1002/1521-3838\(200012\)19:6%3C599::AID-QSAR599%3E3.0.CO;2-B](https://doi.org/10.1002/1521-3838(200012)19:6%3C599::AID-QSAR599%3E3.0.CO;2-B).
  50. Rahman, M.M.; Biswas, S.; Islam, K.J.; Paul, A.S.; Mahato, S.K.; Ali, M.A.; Halim, M.A. Antiviral phytochemicals as potent inhibitors against NS3 protease of dengue virus. *Computers in Biology and Medicine* **2021**, *134*, 104492, <https://doi.org/10.1016/j.compbiomed.2021.104492>.